RSC Advances

ROYAL SOCIETY OF CHEMISTRY

www.rsc.org/advances

Obtaining novel crystalline/amorphous core/shell structure in the barium titanate nanocrystals by an innovative one-step approach

Rouholah Ashiri*

Department of Materials Science and Engineering, Dezful branch, Islamic Azad University, P.O. Box 313, Dezful, Iran

Abstract:

Synthesis temperature and purity of core/shell nanocrystals are key challenges facing the scientific community. Moreover, the core/shell structures usually need a multi-step synthesis pathway to be fabricated. This work aims to address these challenges by developing an innovative one-step synthesis pathway for obtaining carbonate-free $BaTiO_3$ core/shell nanocrystals at low temperature. The results show that very fine $BaTiO_3$ core/shell nanocrystals (<11 nm) free from any by-products such as $BaTi_2O_5$ and $BaCO_3$ are synthesized at 323 K (50 °C). This newly developed structure can significantly reduce the sintering temperature of the nanocrystals and can be beneficial in fabricating the ceramic parts at lower sintering temperatures.

Keywords: Core/shell nanocrystals; One-step synthesis; Carbonate-free; Barium titanate.

* Corresponding author Tel.: +98 9166447795; Fax: +98 6416260890

Email address: ro_ashiri@yahoo.com

1. Introduction

Recent developments in microelectronics, communications and integrated optics have led to the miniaturization of the related devices. Moreover, rapid development of the electronic devices toward miniaturization requires reaching higher performances in smaller structures [1-4]. To fabricate and develop the high-quality volume efficient devices, small particle size nanocrystals with narrow size distribution and high purity are needed [5-6]. Since nanocrystals display a key role in manufacturing the bulk nanostructured electronic devices, therefore economic consideration of mass production of nanocrystals is a major issue concerning the research and development [7, 8].

Recently, nanoscale ferroelectric materials have received considerable attention due to their potential applications in microelectronic, communication and integrated optic technologies [9-11]. Barium titanate ($BaTiO_3$; BTO) is the most common perovskite ferroelectric material, which has been studied extensively because of its wide band gap and outstanding dielectric and ferroelectric properties [5-11]. The successful synthesis of BTO nanocrystals with unique dielectric properties largely depends on the purity and microstructural characteristics, which in turn are dependent on the preparation method. A large number of researches regarding the synthesis of nanoscale BTO crystals using different synthesis methods are available in the literature [5-19].The BTO synthesis pathways reported in the last years can be divided into (1) solid state reaction methods such as mixed oxide method [18-19], and (2) wet-chemical methods such as sol–gel, precipitation, hydrothermal and sonochemical processing methods [5-17, 20-23]. In both groups, considerable progress has been made but it still remains a challenge for the scientific community to obtain high-quality BTO nanocrystals at a low temperature of 323 K (50 °C) while avoiding unwanted by-products. The dielectric properties of BTO are largely affected by carbonates, which

significantly change its dielectric behavior and turn dielectric nature of BTO to semiconducting one [21].

Facile strategies for nanocrystals synthesis are of fundamental importance in the advancement of nanoscience and nanotechnology. In this work, it has been tried to develop and describe a new methodology for the synthesis of carbonate-free BTO nanocrystals. This methodology provides a one-step, convenient, low-cost, nontoxic, and mass-productive route for the synthesis of BTO nanocrystals. On the other hand, BTO is conventionally obtained by solid-state synthesis between barium carbonate ($BaCO_3$) and titania (TiO_2) at 1473 K (1200°C) [18-19]. Some wet chemical approaches need a calcination process at temperatures above 973 K (700°C) [11]. The products of these methods contain some inhomogenities and by-products [13, 16]. As the great advance made by this work, our method of synthesis is able to obtain high-quality homogenous carbonate-free BTO nanocrystals at a low temperature of 323 K (50 °C).

Core-shell nanostructures have recently received much attention for their enhanced properties and performances [24-27]. Moreover, the core–shell structures are normally chosen believing that these can cause a better coupling between the two phases. In this work, a new family of core-shell structure is developed which the core and shell have similar composition while core are crystalline and shell is amorphous. Moreover, for the first time, the novel core/shell nanostructures are obtained by a one-step synthesis method. On theother hand, obtaining nanocrystalline ceramic parts from their nanopowders is one of the most important challenges facing the scientific communities since the high temperature of the sintering process results in particle growth and as the consequence; the final structure becomes submicron-sized. When the shell is amorphous, this layer absorbs thermal energy to become crystalline and thus the required energy for particle growth cannot be provided. The

amorphous shell also can guarantee the higher density of the sintered nanostructured parts at lower sintering temperature.

2. Experimental procedure

2.1. Materials and synthesis method

Our approach is based on an ultrasound assisted wet chemical method. Titanium chloride, barium chloride, anhydrous sodium hydroxide and ethanol are obtained from Merck and used as precursors. The chemicals in the experiment are all analytical grade reagents and used without further treatment. The stoichiometric amounts of barium chloride and titanium chloride are dissolved in deionized water and ethanol, respectively. These solutions are added into a glass vessel containing sodium hydroxide solution. The concentration of the NaOH solution was required to guarantee a strong alkaline environment (pH ≈14) during reaction time. The glass vessel containing precursor solution is subjected to an ultrasonic bath (Soner 220H, 53 kHz, 500 W) at 50 °C for different mixing times. After the reaction is finished and cooled down to room temperature, products are separated and washed followed by drying in an oven at 373 K (100 °C) for 2h. In this work, in order to prevent the unwanted reactions and thus unwanted by-products, we have tried to remove the carbon atom, carbon species and dissolved CO_2 gas in the precursor solution before ultrasound irradiation. We also have tried to prevent the formation of the carbonate phases during sonication. In this way, the above-described method is modified in order to synthesize carbonate-free BTO nanocrystals and the next steps are followed:

i. removal of the carbon species and dissolved CO_2 gas from the deionized water.
ii. preventing the formation of carbonates during sonication (reaction).
iii. dissolution of (possible) formed carbonate by-products from the synthesized products.

In stage (i), the decarbonation treatments of deionized water are performed in three stages including boiling at 373 K (100 °C) for 30 min, bubbling with Ar gas for 30 min and increasing the pH of deionized water above pH 8.5. This three-stage process leads to removal of the carbon species and dissolved CO_2 gas from the deionized water. In stage (ii), during the sonication, the vessel is closed in order to prevent the solution exposing to air and its reaction with CO_2 gas. In stage (iii), after reaction is finished and cooled to room temperature, the precipitates are separated from the reaction mixture, and washed four times with deionized water, diluted formic acid, diluted hydrochloric acid and ethanol, respectively. The washing process is done in order to dissolve the (possible) formed carbonate by-products from the synthesized products. BTO nanocrystals are prepared at 323 K (50 °C) using the method described above.

2.2. Characterization

Functional groups in the product are detected using a FT-IR spectrophotometer (Hitachi 3140; Tokyo, Japan). FT-IR spectrum is recorded in the range of 400–4000 cm^{-1} and measured on samples in KBr pellets. The crystal structure of the obtained powder products is determined using an X-ray diffractometer (Philips PW3710; Eindhoven, the Netherlands). The average crystallite size of the products is calculated using Scherrer's formula [22]. The morphological features and microstructure of the products are observed by a field emission scanning electron microscope (FE-SEM; Hitachi S4160) and high-resolution transmission electron microscope (HRTEM; ZEISS EM900). All of the characterizations were performed at room temperature.

3. Results and discussion

3.1. Structure, purity and formation mechanism of the obtained powder products

FT-IR is known as a sensitive technique for carbonate phase identification. Fig. 1a shows FT-IR spectrum of the synthesized nanocrystals. FT-IR spectrum reveals the presence of absorption bands at around 539, 1435, 1582 and 3441 cm^{-1}. The absorption bands at 3441 and 1582 cm^{-1} are assigned to O-H stretching and bending vibrations of water [23]. The absorption bands at 1435 cm^{-1} can be considered as the alcoholic bending vibrations (C-OH functional groups) [23] implying the adsorption of small amount of alcohol on the surface of nanocrystals. These absorptions are due to the use of ethanol in the washing process of the as-synthesized nanocrystals. Strong and wide band located between 780 and 470 cm^{-1} can be ascribed to BTO stretching vibrations and confirms the formation of BTO. This band is a combination of the following bands: a band at 652 cm^{-1} which is assigned to stretching vibrations of BaO and a band at 470 cm^{-1} which is assigned to stretching vibrations of TiO_2 [23]. Since the characteristic bands of the carbonates (867, 1049, 1421 cm^{-1}) [23] have not been appeared in our spectrum, it can be stated that the synthesized nanocrystals are carbonate-free and thus highly pure. This outcome is the significant advantage of the present method in contrast to other established methods [5-19].

XRD results (Fig. 1b) also indicate that the method leads to formation of the carbonate-free BTO nanoscale crystals with perovskite symmetry. BTO nanocrystals are characterized by well-resolved peaks at 22.04, 31.45, 38.66, 44.97, 50.60, 55.91, 65.42, 69.94 and 74.21° corresponding to the (1 0 0), (1 1 0), (1 1 1), (2 0 0), (2 1 0), (2 1 1), (2 2 0), (2 1 2) and (3 1 0) planes. All peaks of the XRD pattern match well with standard cubic BTO perovskite phase JCPDS No. 31-174 confirming the formation of BTO with perovskite symmetry. The XRD pattern of the synthesized product is consistent with other reports [5-6]. Considering the prominent (1 1 0) peak and using the Scherrer formula given in Ref. [22], we estimate the average crystallite size of the synthesized product to be 10.1 nm. In this pattern, the halo pattern is also pronounced due to existence of amorphous phase. On the other hand, the peaks

of carbonate phases (which are normally seen at 23.52, 25.04, 33.92, 41.88, 46.6, 53.68, 68.04° [22-23]) are not found in the pattern of Fig. 1b, therefore, it can be said that the product is carbonate-free. The above results indicate that very fine BTO nanocrystals free from any by-product have been obtained through the present synthesis pathway.

The above-described method has several advantages over other sonochemical routes [17, 28-30] and even over other processing methods, such as sol-gel [11], solid-state reaction [18-19], combustion synthesis [31], co-precipitation [13, 15], hydrothermal [9] and microemulsion [32] methods. In contrast to other sonochemical processes [17, 28-30], for the first time, carbonate-free BTO nanocrystals have been prepared in this work. Moreover, the products are synthesized at a lower temperature in contrast to the literature [17, 28-30]. Other researchers [17, 28-30] have indicated that a temperature above 363 K (90 °C) is required for sonochemical synthesis of BTO nanocrystals, but in this work, carbonate-free BTO nanocrystals are synthesized at 323 K (50 °C). Moreover, this temperature is much lower than the temperature required for other processing methods [5-17, 18-19, 21-22]. This advantage indicates that the established method is cost-effective, and therefore suitable for mass production purposes. Here, we explain the mechanism of formation of BTO nanocrystals and discuss the above-mentioned results. In the sonochemical processing method, ultrasonic waves radiate through the precursor solution causing alternating high and low pressures in the solution. This leads to the formation, growth, and implosive collapse of bubbles in the solution. These conditions greatly accelerate the rate of the formation of the products without need for any additional external heating. The formation mechanism of the synthesized nanocrystals is related to radicals involved in the reaction because of the bubble's collapse. According to hot spot theory [33], very high temperatures (> 5273 K (5000 °C)) and pressures of roughly 2000 atm are obtained upon the collapse of a bubble. Since this collapse occurs in less than a nanosecond, very high cooling rates (>1010 K/s) are also obtained. These extreme

conditions can drive a variety of chemical reactions to fabricate nano-sized materials. In other words, the implosion of the microscopic bubbles in the reaction mixture generates energy, which induces chemical and mechanical effects [23]. This collapse leads to localization, a transient high temperature and pressures, resulting in an oxidative environment due to the generation of highly reactive species, including hydroxyl radical (˙OH) [33]. These radicals are formed in the reaction mixture due to the use of deionized water and alcohol as precursors. On the other hand, this oxidative environment provides suitable conditions for the formation of the oxide nanocrystal. The reaction pattern for the formation of the BTO nanocrystals is as follows:

$$BaCl_2(aq) + TiCl_4(aq) + 6NaOH(aq) \xrightarrow{\text{Ultrasonic irradiation at 50 °C}} \mathbf{BaTiO_3}(s) + 6NaCl(aq) + 3H_2O(l) \quad (1)$$

where (*aq*) denotes a salt dissolved in deionized water and (*s*) denotes the synthesized precipitates. $BaTiO_3$ (BTO) is the main product of the above reaction pattern exhibiting the perovskite symmetry. Nevertheless, such high temperatures and pressures can activate existing carbon atoms, carbon species and dissolved CO_2 gas (in the precursor solution) for chemical reactions to form carbonate by-products (carbonate phases). This event is the reason behind the fact that other researchers were not successful in synthesizing carbonate-free BTO [17, 28-30]. It seems that the removal of carbon species and dissolved CO_2 gas from the precursor solution (as described in the experimental procedure) is effective in reducing the synthesis temperature and leads to formation of the carbonate-free BTO nanocrystals at a lower temperature in contrast to the previous reports [17, 28-30]. In addition, it can be discussed that the formation of BCO (barium carbonate oxide; barium carbonate) or other carbonate by-products postpones the formation of BTO. BCO is thermodynamically more stable than BTO [22], it is formed at a lower temperature in contrast to BTO. Therefore, in the presence of free carbon, carbon species and dissolved CO_2 gas in the reaction chamber, BCO

formation is preferred, especially in the ultrasound-assisted synthesis due to severe temperature and pressure conditions discussed before [33]. On the other hand, after the decomposition of BCO, BTO is formed according to the following reactions:

$$BaCO_3 \rightarrow BaO + CO_2 \quad (2)$$

$$BaO + TiO_2 \rightarrow BaTiO_3 \quad (3)$$

Therefore, it can be said that with increasing amount of the carbonate phases, formed during the synthesis, the formation of BTO is delayed. Consequently, we designed our method considering these facts and the mentioned three steps (in the experimental section) were followed to remove free carbon atoms, carbon species and dissolved CO_2 gas from the precursor solution before the irradiation of the ultrasound waves. The applied modifications also prevent unwanted reactions between CO_2 gas and precursor solution during sonication. These condition leads to formation of carbonate-free BTO nanocrystals.

3.2. Microstructure, morphology and formation mechanism of the obtained powder products

Fig. 2 shows FE-SEM and TEM micrographs and SAED pattern of BTO powder product. As can be seen in the FE-SEM micrographs, the powders appear to be agglomerated caused primarily by the processes occurring during drying of the as-synthesized powders. Moreover, small particles embedded in each agglomerated cluster correspond to the BTO nanocrystals. All the FE-SEM micrographs exhibit particles greater than the average crystallite size determined by the analysis of XRD, suggesting an internal structure of the particles. The curves of the particle size distribution of the synthesized BTO samples with different sonication times have been shown in Fig. 3. The particle size seen in these curve is much larger than the size of crystallites estimated by Scherrer equation suggesting an internal structure of the particles. The curve of the sample sonicated for 45 min indicates that the

particles are generally composed of 2-10 crystallites but most of them are composed of 4-6 crystallites. The morphological properties and size distribution characterization of the prepared powders indicate that the products consist of somewhat regularly shaped and relatively spherical particles with a narrow size distribution. The above results indicated that with the help of ultrasound irradiation, carbonate-free BTO particles with tailored morphology can be synthesized using our established method. Moreover, the ultrasonication accelerates the homogeneous precipitation process and can also be beneficial in controlling the size and shape of the synthesized nanocrystals. It is apparent from the FE-SEM micrographs that the BTO nanocrystals appearing in the agglomerates are relatively uniform in size having spherical morphology. There are some other papers describing synthesis of BTO without sonication; those methods produce poorly uniform particles with board particles size distributions [5-8] at much higher temperatures. However, the results indicate that with the help of ultrasound irradiation, we can obtain monosized particles with spherical morphology at much lower temperatures in contrast to the literature [5-19].

Fig. 2 also shows the HRTEM micrographs at different magnifications and SAED pattern of the BTO nanopowders synthesized in this work. These micrographs show BTO nanocrystals and nanometric agglomerates, and prove the nanocrystalline structure of the synthesized BTO. Moreover, the crystallite size of particles is in good agreement with the data obtained from the Scherrer formula. TEM micrographs also show a halo shell around the obtained nanocrystals. This indicates that the obtained nanosized crystals have an internal crystalline/amorphous core/shell structure. The selected area electron diffraction (SAED) pattern exhibits hazy circles at the center, which indicates the product is nanocrystalline. This pattern also shows the presence of concentric rings confirming the polycrystallinity of the agglomerates. The sonochemical processing method used in this work leads to the homogeneous precipitation of non-agglomerated BTO nanocrystals at the end of the synthesis

process. Then the precipitates are separated, washed, and then dried in an oven at 373 K (100 °C) for 2h. As can be seen in Fig. 2, the dried nanopowders are seen as agglomerates composed by BTO nanocrystals. However, they are loose agglomerates and can be dispersed in aqueous medium without needing a grinding step. Moreover, the better clear HRTEM micrograph (Fig. 2) clearly shows the contacted areas of the nanocrystals indicating the nanocrystals have been agglomerated together with weak forces during drying stage of the as-synthesized precipitates.

During sonication, ultrasonic waves radiate through the precursor solution causing alternating high and low pressures in the solution. This leads to the formation, growth, and implosive collapse of bubbles in the solution (see Fig. 4). The collapse of bubbles with short lifetimes produces intense local heating and high pressure. According to hot spot theory [33], very high temperatures (> 5273 K (5000 °C)) and pressures of roughly 2000 atm are obtained upon the collapse of a bubble. Since this collapse occurs in less than a nanosecond, very high cooling rates (>1010 K/s) are also obtained. These extreme conditions can drive a variety of chemical reactions to fabricate nano-sized materials. Since these events occur in localized discrete points (at the collapsing bubbles), therefore sonochemical processing method leads to formation of the nanocrystals. But, as can be seen in SEM and TEM micrographs, the synthesized powders appear to be agglomerated. This caused primarily by the processes occurring during the drying stage of the as-synthesized powders and small particles embedded in each agglomerated cluster correspond to the synthesized nanocrystals. In this work, the products have been synthesized at 323 K (50 ºC). Moreover, the nanocrystals were not subjected to a calcining process at high temperature which leads to formation of highly agglomerated almost inseparable particles. Therefore, it can be said that the nanocrystals have been aggregated together with weak forces. In TEM micrographs (see Fig. 2), the contacted

areas of the nanocrystals are seen which indicates that the nanocrystals have been aggregated together with weak forces during drying stage of the as-synthesized precipitates.

TEM micrographs also show a halo shell around the obtained nanocrystals. In analysis of this result, it can be said that the extremely high localized pressures and temperatures induced by ultrasound irradiation at collapsing bubbles remain for less than one nanosecond and therefore very high cooling rates (>1010 K/s) are obtained [33] due to self-quenching effect of the precursor solution. Such high cooling rates prevent growth of the forming nanocrystals and lead to formation of a crystalline/amorphous core/shell structure in the synthesized nanocrystals. This structure has been clearly presented in Fig. 5. It seems to us that this structure can significantly reduce the sintering temperature of the obtained powder. Here, we explain the role of the application of ultrasound irradiation on the formation of a crystalline/amorphous core/shell structure in the obtained nanocrystals. When precursor solution is exposed to ultrasound irradiation, the bubbles are implosively collapsed by acoustic fields in the solution.

Here, we explain our proposed mechanism of formation of the crystalline/ amorphous core/shell nanostructures. There are two regions of sonochemical activity (see Fig. 4) upon the collapse of a bubble. One is inside of the collapsing bubbles, where elevated temperatures (> 5273 K (5000 °C)) and high pressures (roughly 2000 atm) are produced and can result in the formation of the crystalline core of the crystalline/ amorphous core/shell nanostructures; the other is interfacial region between the cavitation bubbles and surrounding solution [33]. The temperature in the interfacial region is much lower than the inside of the collapsing bubbles, but it is still high enough to rupture chemical bonds and induce many reactions without need for any external heating. This effect and very high cooling rates occurring in the sonochemical processing method freeze the ordering transformation in the amorphous shell and leads to formation of a crystalline/amorphous core/shell structure (see Fig. 6). Actually,

the collapse of bubbles (acoustic cavitation due to the ultrasonication of the reaction mixture) has also mechanical effects. In other words, as the third effect, the microscopic stirring can also be obtained through the collapse of bubbles. The nanostructures are obtained due to the high temperatures and pressures in very local area and the microscopic stirring induced by these cavitations modifies the shape of the forming nanocrystals to be regular and mostly spherical. These three effects induced by ultrasonication result in obtaining spherical amorphous/crystalline core/shell nanostructures in this work. The formed core/shell nanostructures grow with the synthesis time in the following way: in the first step, transformation of amorphous shell to crystalline phase occurs, in the second step a new amorphous shell is formed on the growing crystalline core (these two steps can be simultaneous). Progress of the growth of the nanostructures is the result of repetition of these two steps. Since these conditions exist in any sonochemical processing method, sonochemical processing method is the best option to obtain such core/shell nanostructures by a facile one-step synthesis pathway. It seems to us that this structure can significantly reduce the sintering temperature of the obtained powders and can be beneficial in fabrication ceramic parts at lower sintering temperatures.

4. Conclusions

In this work, we reported an one-step approach for synthesizing BTO crystalline/amorphous core/shell nanocrystals. The method is a novel ultrasound-assisted wet chemical synthesis. Well-defined and stoichiometric nanocrystals of BTO of narrow size distribution were synthesized at 323 K (50 °C) by sonication of chloride solution in a strong alkaline environment. The mechanism of formation of the crystalline/ amorphous core/shell nanostructures was disclosed in the text. The method allows a tailor-made preparation of the

powder particles. Moreover, the preparation of nanocrystals, described here, is simple, fast, inexpensive and useful for large-scale production purposes.

References

[1] V. Buscaglia, M.T. Buscaglia, M. Viviani, L. Mitoseriu, P. Nanni, V. Trefiletti, Grain size and grain boundary-related effects on the properties of nanocrystalline barium titanate ceramics, J. Eur. Ceram. Soc. 26 (2006) 2889–2898.

[2] M. Niederberger, N. Pinna, J. Polleux, M. Antonietti, A general soft-chemistry route to perovskites and related materials: Synthesis of $BaTiO_3$, $BaZrO_3$, and $LiNbO_3$ nanoparticles, Angew. Chemie. 43 (2004) 2270–2273.

[3] X. Zheng, S. Tan, L. Dong, S. Li, H. Chen, $LaNiO_3$@ SiO_2 core–shell nano-particles for the dry reforming of CH_4 in the dielectric barrier discharge plasma, Int. J. Hydrogen. Energ. 39 (2014) 11360-11367.

[4] L. Zhang, D. Zhang, J. Zhang, S. Cai, C. Fang, L. Huang, H. Li, R. Gao, L. Shi, Design of meso-TiO_2@ MnO_x–CeO_x/CNTs with a core–shell structure as $DeNO_x$ catalysts: promotion of activity, stability and SO_2-tolerance, Nanoscale. 5 (2013) 9821-9829.

[5] X. Zhu, J. Wang, Zh. Zhang, J. Zhu, Sh. Zhou, Zh. Liu, N. Ming, Atomic-Scale Characterization of Barium Titanate Powders Formed by the Hydrothermal Process, J. Am. Ceram. Soc. 91 (2008) 1002–1008.

[6] S. Yoon, K. Kim, S. Baik, The Route for Synthesis of Agglomeration-Free Barium Strontium Titanate Nanoparticles Using Ultrasonic Spray Nozzle System, J. Am. Ceram. Soc. 93 (2010) 998–1002.

[7] X. He, J. Ouyang, J. Jin, H. Yang, Rapid synthesis of barium titanate microcubes using composite-hydroxides-mediated avenue, Mater. Res. Bull. 52 (2014) 108–111.

[8] Y. Xie, Sh. Yin, T. Hashimoto, Y. Tokano, A. Sasaki, T. Sato, Low temperature synthesis of tetragonal $BaTiO_3$ by a novel composite-hydroxide-mediated approach and its dielectric properties, J. Euro. Ceram. Soc. 30 (2010) 699–704.

[9] W. Wang, L. Caon, W. Liu,G. Su,W. Zhang, Low-temperature synthesisof$BaTiO_3$ powders bythesol–gel-hydrothermal method, Ceram. Inter. 39 (2013) 7127–7134.

[10] T. M. Stawski, S. A. Veldhuis, O. F. Gobel, J. E. Elshof, D. H. A. Blank, Effects of Reaction Medium on the Phase Synthesis and Particle Size Evolution of $BaTiO_3$, J. Am. Ceram. Soc. 93 (2010) 3443–3448.

[11] U.-Y. Hwang, H.-S. Park, K.-K. Koo, Low-Temperature Synthesis of Fully Crystallized Spherical $BaTiO_3$ Particles by the Gel–Sol Method, J. Am. Ceram. Soc. 87 (2004) 2168–2174.

[12] X. Chen, Ch. Fang, Study of electrocaloric effect in barium titanate nanoparticle with core–shell model, Physica B415 (2013) 14–17.

[13] S. Yoon, S. Baik, M. G. Kim, N. Shin, Formation Mechanisms of Tetragonal Barium Titanate Nanoparticles in Alkoxide–Hydroxide Sol-Precipitation Synthesis, J. Am. Ceram. Soc. 89 (2006) 1816–1821.

[14] J. Cao, Y. Ji, Ch. Tian, Zh. Yi, Synthesis and enhancement of visible light activities of nitrogen-doped $BaTiO_3$, J. Allo. Compd. 615 (2014) 243–248.

[15] P. Pinceloup, Ch. Courtois, A. Leriche, B. Thierry, Hydrothermal Synthesis of Nanometer-Sized Barium Titanate Powders: Control of Barium/Titanium Ratio, Sintering, and Dielectric Properties, J. Am. Ceram. Soc. 82 (1999) 3049–3056.

[16] Q. Feng, M. Hirasawa, K. Kajiyoshi, K. Yanagisawa, Hydrothermal Soft Chemical Synthesis and Particle Morphology Control of $BaTiO_3$ in Surfactant Solutions, J. Am. Ceram. Soc. 88 (2005) 1415–1420.

[17] M. Xu, Y.-N. Lu, Y.-F. Liu, S.-Z. Shi, T.-S. Qian, D.-Y. Lu, Sonochemical synthesis of monosized spherical $BaTiO_3$ particles, Powder Tech. 161 (2006) 185-189.

[18] Y. Hotta, K. Tsunekawa, T. Isobe, K. Sato, K. Watari, Synthesis of $BaTiO_3$ powders by a ball milling-assisted hydrothermal reaction, Mater. Sci. Eng. A 475 (2008) 12–16.

[19] A.C. Roy, D. Mohanta, Structural and ferroelectric properties of solid-state derived carbonate-free barium titanate ($BaTiO_3$) nanoscale particles, Scripta Mater. 61 (2009) 891-894.

[20] R. Ashiri, Analysis and characterization of relationships between the processing and optical responses of amorphous $BaTiO_3$ nanothin films obtained by an improved wet chemical process, Metall. Mater. Trans. B45 (2014) 1472-1483.

[21] R. Ashiri, A. Nemati, M. Sasani Ghamsari, Crack-free nanostructured BaTiO3 thin films prepared by sol–gel dip-coating technique, Ceram. Int. 40 (2014) 8613-8619.

[22] R.Ashiri, A Mechanistic study of nanoscale structure development, phase transition, morphology evolution, and growth of ultrathin barium titanate nanostructured films, Metall. Mat. Trans. A45 (2014) 4138-4154.

[23] R. Ashiri, Detailed FT-IR spectroscopy characterization and thermal analysis of synthesis of barium titanate nanoscale particles through a newly developed process. Vib. Spec. 66 (2013) 24-29.

[24] R. França, X-F. Zhang, T. Veres, L. Yahia, E. Sacher, Core–shell nanoparticles as prodrugs: Possible cytotoxicological and biomedical impacts of batch-to-batch inconsistencies, J. Colloid. Interf. Sci. 389 (2013) 292-297.

[25] D. Zhang, T. Yan, L. Shi, C. Pan, J. Zhang, Ethylene glycol reflux synthesis of carbon nanotube/ceria core–shell nanowires, Appl. Surf. Sci. 255 (2009) 5789-5794.

[26] D. Rosario-Amorin, M. Gaboyard, R. Clérac, L. Vellutini, S. Nlate, K. Heuzé, Metallodendritic grafted core–Shell γ-Fe_2O_3 nanoparticles used as recoverable catalysts in Suzuki C-C coupling reactions, Chem.-Eur. J. 18 (2012) 3305-3315.

[27] D. Zhang, X. He, H. Yang, L. Shi, J. Fang, Surfactant-assisted reflux synthesis, characterization and formation mechanism of carbon nanotube/europium hydroxide core-shell nanowires, Appl. Surf .Sci. 255 (2009) 8270-8275.

[28] S. Vuttivong, S. Niemcharoen, P. Seeharaj, W. C. Vittayakorn, N. Vittayakorn, Sonochemical synthesis of spherical $BaTiO_3$ nanoparticles, Ferroelectrics 457 (2013) 44-52.

[29] F. Dang, K. Kato, H. Imai, S. Wada, H. Haneda, M. Kuwabara, A new effect of ultrasonication on the formation of $BaTiO_3$ nanoparticles, Ultrason. Sonochem. 17 (2010) 310-314.

[30] F. Dang, K. Kato, H. Imai, S. Wada, H. Haneda, M. Kuwabara, Growth of $BaTiO_3$ nanoparticles in ethanol-water mixture solvent under an ultrasound-assisted synthesis, Chem. Eng. J. 170 (2011) 333-337.

[31] T.V. Anuradha, S. Ranganathan, T. Mimani, K.C. Patil, Combustion synthesis of nanostructured barium titanate, Scripta Mater. 44 (2001) 2237–2241.

[32] C. Pithan, Y. Shiratori, R. Waser, Preparation, processing, and characterization of nano-crystalline $BaTiO_3$ powders and ceramics derived from microemulsion-mediated synthesis, J. Am. Ceram. Soc. 89 (2006) 2908-2916.

[33] T. J Mason, J. P. Lolimer, Applied Sonochemistry, Wiley-VCH Verlag, U.K., 2002.

Figure captions

Fig. 1. (a) FT-IR spectrum and (b) XRD pattern of BTO nanocrystals synthesized through our established method.

Fig. 2. FE-SEM and TEM micrographs at different magnifications, and SAED pattern of BTO nanocrystals synthesized in this work.

Fig. 3. The change of particle size distribution of the synthesized powder products with sonication time.

Fig. 4. The schematic illustration showing the formation, growth, and collapse of a bubble induced by ultrasonication.

Fig. 5. HRTEM micrograph showing the formation of a crystalline/amorphous core/shell structure in the BTO nanocrystals synthesized in this work.

Fig. 6. The schematic illustration showing the formation mechanism of BTO crystalline/amorphous core/shell nanocrystals induced by ultrasonication.

Figure 1

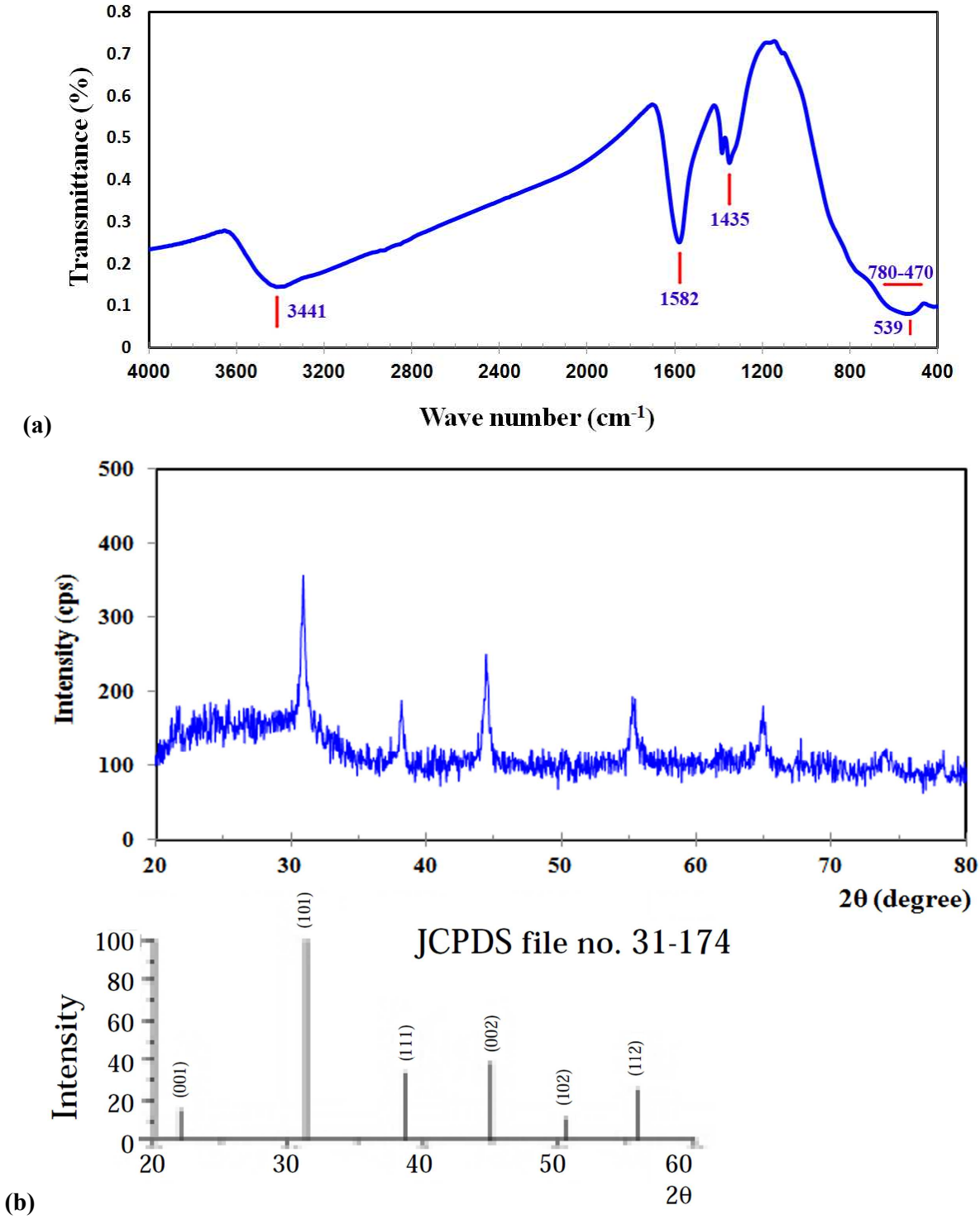

Fig. 1. (a) FT-IR spectrum and (b) XRD pattern of BTO nanocrystals synthesized through our established method.

Figure 2

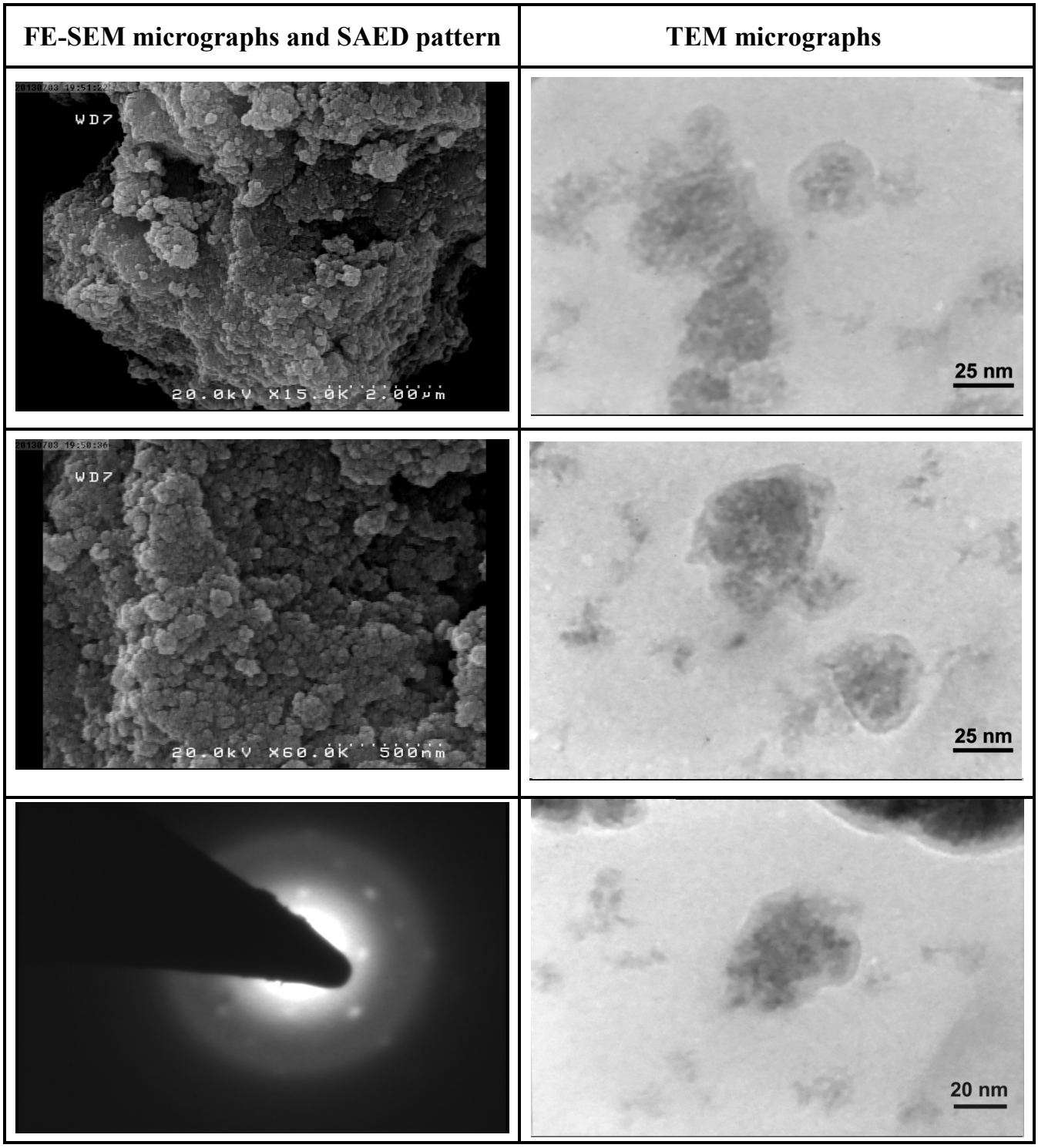

Fig. 2. FE-SEM and TEM micrographs at different magnifications, and SAED pattern of BTO nanocrystals synthesized in this work.

Figure 3

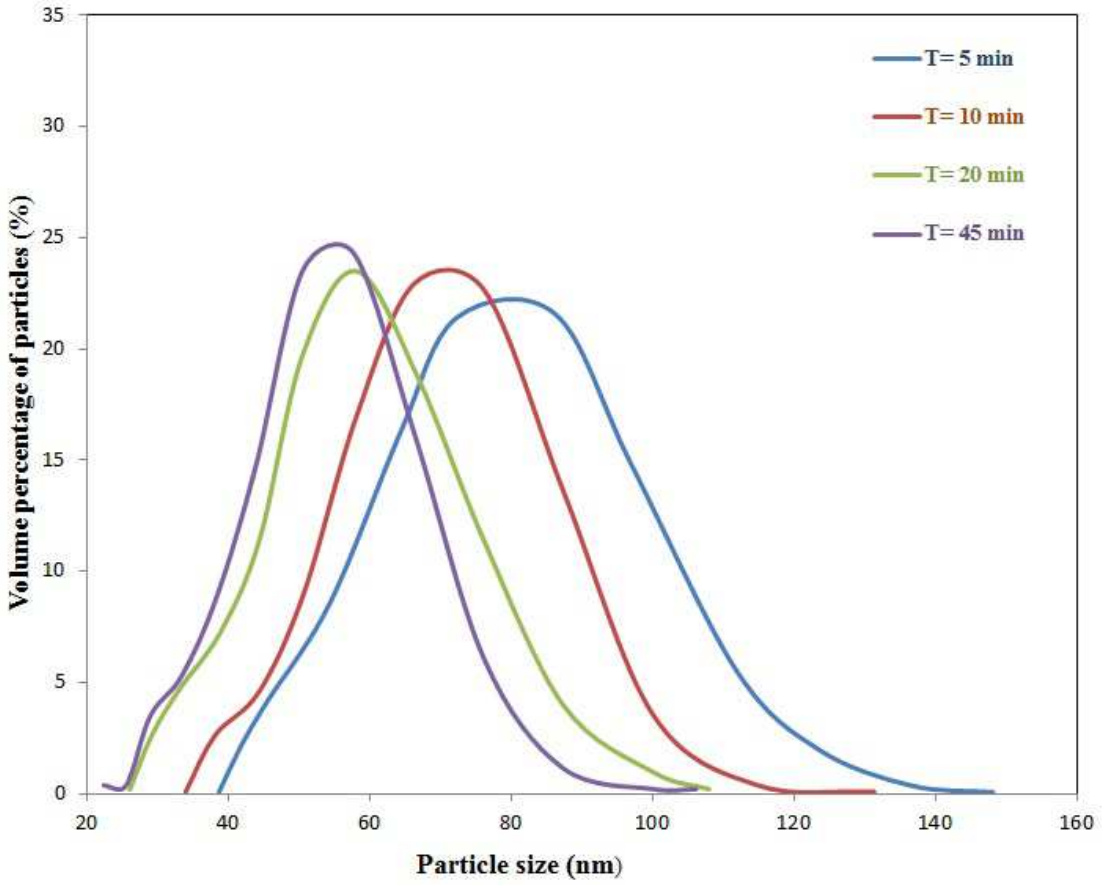

Fig. 3. The change of particle size distribution of the synthesized powder products with sonication time.

Figure 4

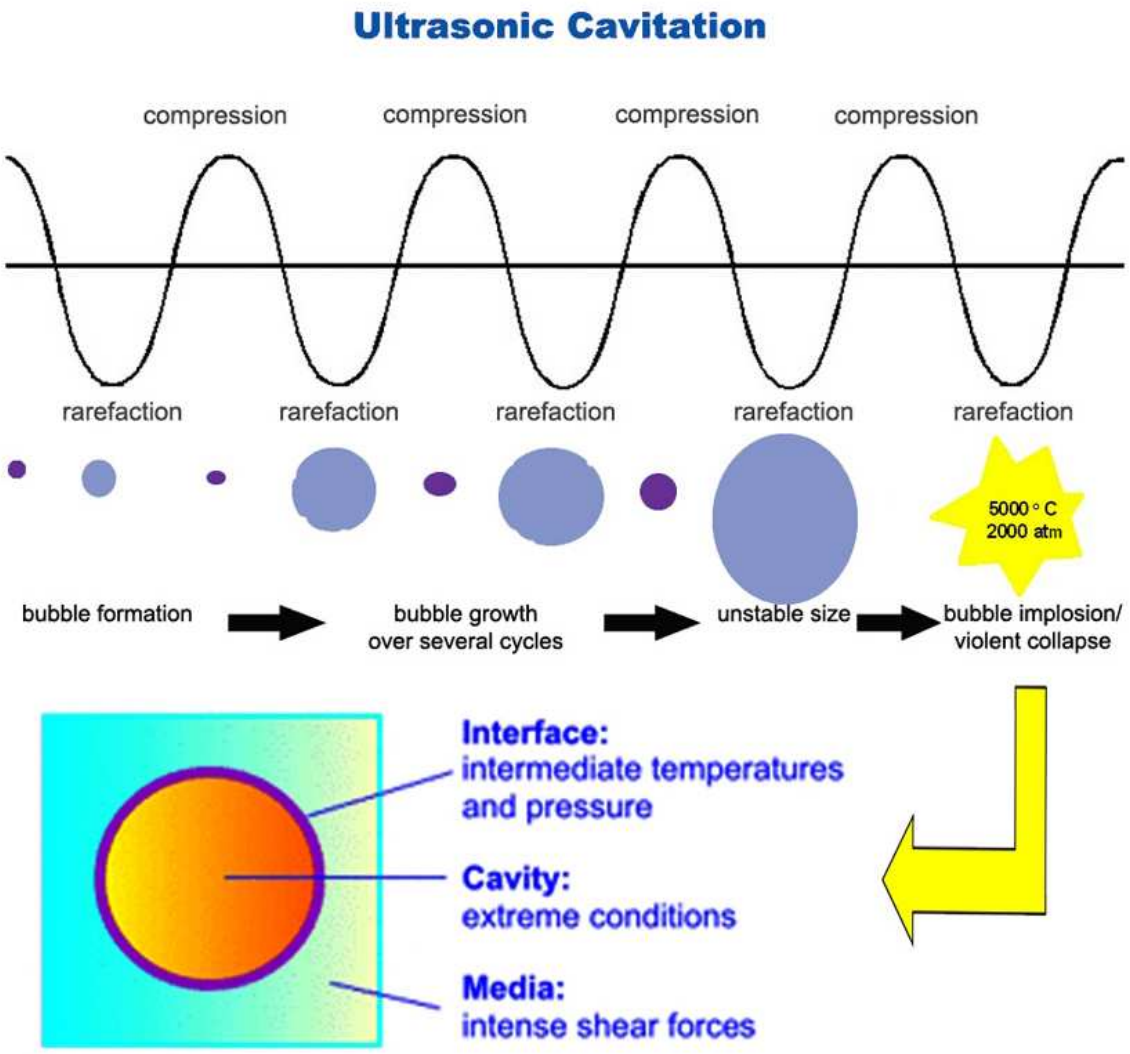

Fig. 4. The schematic illustration showing the formation, growth, and collapse of a bubble induced by ultrasonication.

Figure 5

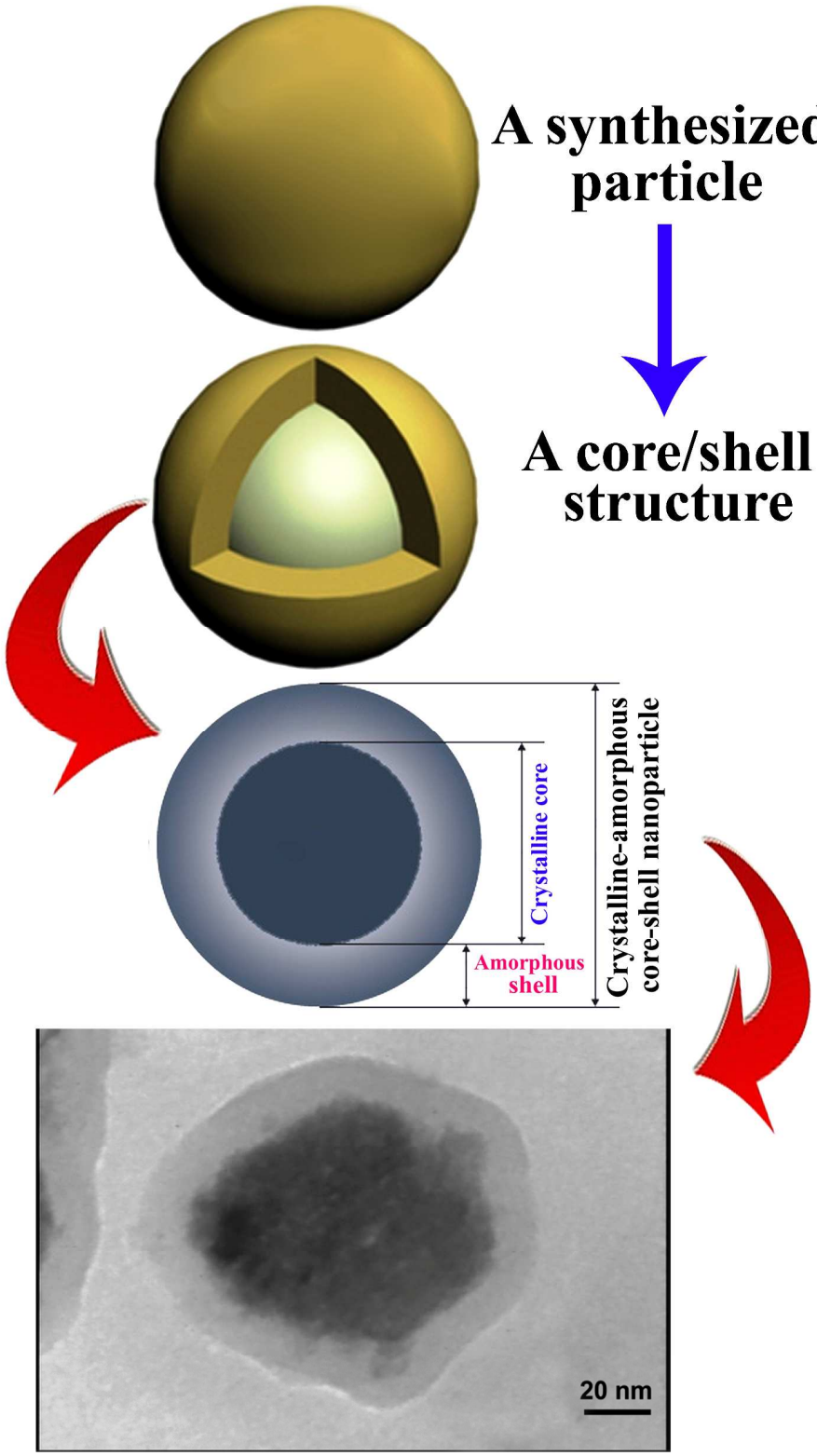

Fig. 5. HRTEM micrograph showing the formation of a crystalline/amorphous core/shell structure in the BTO nanocrystals synthesized in this work.

Figure 6

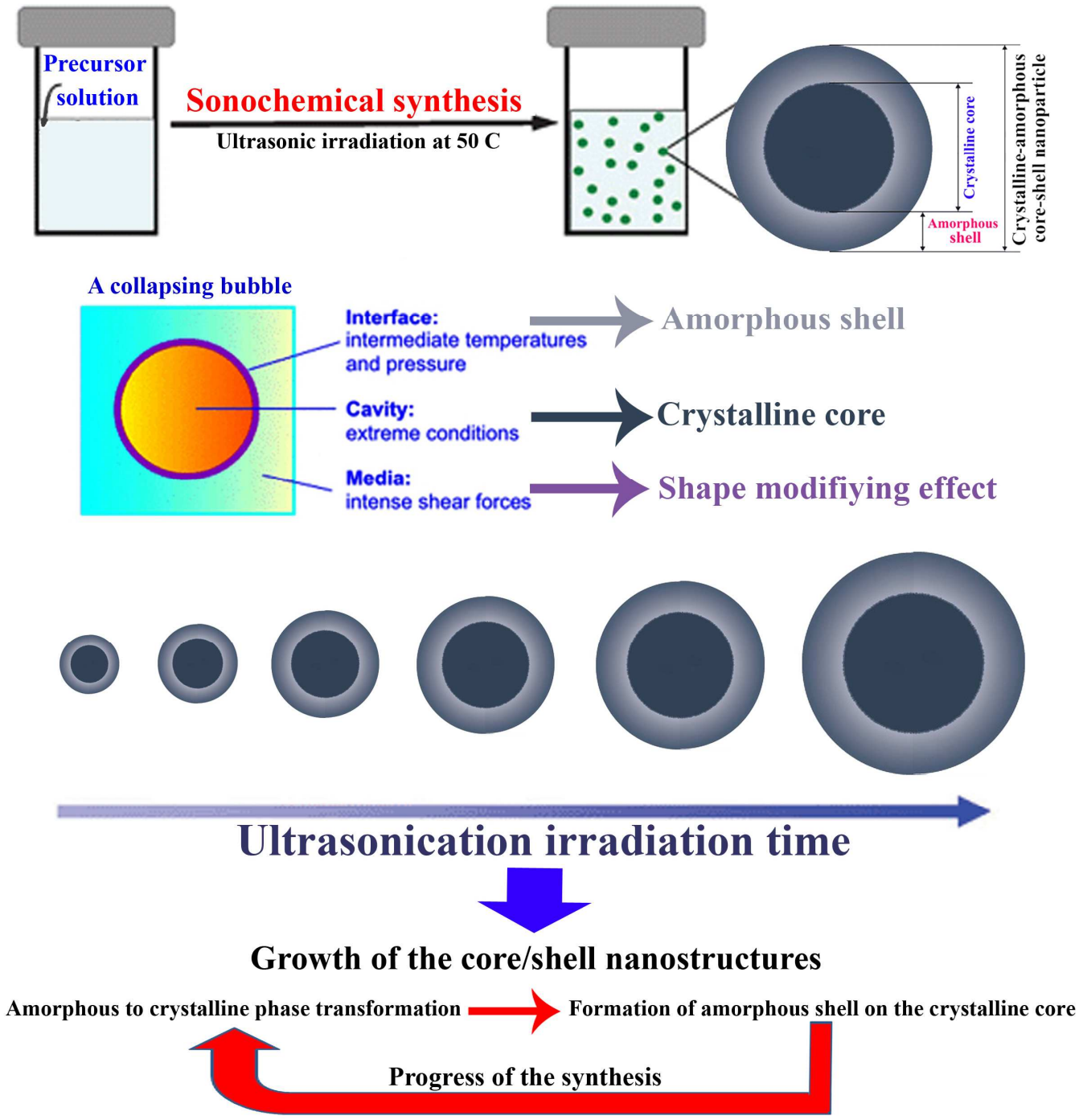

Fig. 6. The schematic illustration showing the formation mechanism of BTO crystalline/amorphous core/shell nanocrystals induced by ultrasonication.